Journal of Applied Physics

RESEARCH ARTICLE | OCTOBER 04 2021

Dual mode operation of a hydromagnetic plasma thruster to achieve tunable thrust and specific impulse

Thomas C. Underwood ✉ ; William M. Riedel ; Mark A. Cappelli

Journal of Applied Physics 130, 133301 (2021)
https://doi.org/10.1063/5.0051467

AIP Publishing

Journal of Applied Physics ARTICLE scitation.org/journal/jap

Dual mode operation of a hydromagnetic plasma thruster to achieve tunable thrust and specific impulse

Cite as: J. Appl. Phys. **130**, 133301 (2021); doi: 10.1063/5.0051467
Submitted: 25 March 2021 · Accepted: 8 September 2021 ·
Published Online: 4 October 2021

Thomas C. Underwood,[1,a] William M. Riedel,[2] and Mark A. Cappelli[2]

AFFILIATIONS

[1]Department of Aerospace Engineering and Engineering Mechanics, University of Texas at Austin, Austin, Texas 78712, USA
[2]Stanford Plasma Physics Laboratory, Mechanical Engineering Department, Stanford University, Stanford, California 94305, USA

Note: This paper is part of the Special Topic on Physics of Electric Propulsion.

[a]**Author to whom correspondence should be addressed:** thomas.underwood@utexas.edu

ABSTRACT

We report here on initial studies of a pulsed hydromagnetic plasma gun that can operate in either a pre-filled or a gas-puff mode on demand. These modes enable agile and responsive performance through tunable thrust and specific impulse. Operation with a molecular nitrogen propellant is demonstrated to show that the hydromagnetic thruster is a candidate technology for air-harvesting and drag compensation in the very low Earth orbit. A dual mode operation is achieved by leveraging propellant gasdynamics to change the fill fraction and flow collisionality within the thruster. This results in the formation of distinct modes that are characterized by the current-driven hydromagnetic waves that they allow, namely, magneto-deflagration and magneto-detonation, respectively. These modes form the basis of using gasdynamics to enable responsive thruster performance. Using time-of-flight emission diagnostics to characterize near-field flow velocities, we find that a relatively dramatic transition occurs between modes as gas is allowed to expand in the thruster, with exhaust velocities ranging from 10 to 55 km/s in the deflagration and detonation regimes, respectively. Simulations of the processed mass bit offer the first glimpse into possible thruster performance and trade-offs between specific impulse and thrust. An impulse bit tunability of ∼22% is predicted, with differing propellant fill fractions when operating in a burst mode.

I. INTRODUCTION

Propulsion technologies continue to be limited by their inability to offer agile and responsive performance. A common example is the trade-off between the efficiency of the propellant usage (specific impulse, I_{sp}) and the generation of thrust (T).[1] In systems ranging from chemical rockets to electric thrusters, any increase in thrust generation is typically accompanied by a decrease in the acceleration efficiency of the propellant. This can constrain the scope of missions and, in some cases, requires the use of multiple propulsion systems to satisfy the required altitude, duration, weight, and level of thrust generation. Increasingly, there is a need for emerging technologies that can rapidly change their operational performance (i.e., T or I_{sp}) in response to changing mission objectives. Added performance agility can allow a single thruster to smoothly transition from optimizing propellant usage to thrust generation while in the orbit.

Electric propulsion (EP) uniquely leverages electromagnetic fields to ionize and accelerate the propellant.[2] This allows EP technology to operate efficiently in applications that demand thrust generation and I_{sp} levels spanning many orders of magnitude. The use of external electrical power also adds a level of control over the operational characteristics of the thruster. For example, depending on the manner in which energy is supplied, EP technology can be categorized as either an electrospray or a plasma-based electrostatic, electromagnetic, or electrothermal thruster. Research into these systems has focused on uncovering mechanisms that enable reliable and sustained operation at either high thrust efficiency (T/P) *or* I_{sp}. Recent work has explored throttability in EP systems by measuring performance trade-offs (i.e., thrust and I_{sp}) with an increasing discharge voltage.[3] More work, needs to be done to explore how new methods can enable reconfigurability in EP systems and how these

methods might allow rapid and on-demand transitions between values of high T/P *and* I_{sp}.

Beyond reconfigurability, simply operating EP systems in different gasdynamic environments is a challenge that has been largely unexplored. Recent efforts[4] to use plasma thrusters in an air-breathing configuration for very low Earth orbit (VLEO) conditions have been met with significant performance decreases. Measurements of the plume composition in a low power Z-70 (500 W) Hall effect thruster (HET) operating on Xe/air mixtures confirm the presence of ions of both molecular and atomic states suggesting that a considerable amount of energy may be invested in dissociation.[5] In recent unpublished studies in our laboratory, the transition from Xe (100%) to $Xe--N_2$ (17%–83%) mixtures in the same Z-70 thruster reduced the thrust from 24 to 13 mN and I_{sp} from 1270 to 820 s for comparable thruster power. It is still uncertain if electrothermal or inductive thruster technology can generate I_{sp} or thrust requirement for the sustained VLEO operation.[6–8] Pulsed plasma thrusters (PPTs) on the other hand have shown the ability to still operate efficiently (exceeding 30%) on molecular propellants such as water vapor[9] or N_2[10] due, in part, to their higher input energies. Experiments have also found that differing levels of propellant loading within PPTs result in distinct operational characteristics.[11,12] Thrust measurements by Ziemer[13] even indicated the presence of anomalously high thrust efficiency when small quantities ($<1\,\mu g$) of the propellant were injected. These observations motivate the exploration of gasdynamic loading in PPTs as a controllable means to enable reconfigurability and agile operation.

This paper describes a novel pulsed hydromagnetic thruster that can operate in two distinct modes. These modes feature distinct time scales, properties, propellant flow requirements, and energy densities that can be leveraged to engineer performance on demand. The first, called magneto-detonation, is a transient mode that enables the selective generation of higher thrust levels. Magneto-detonation is characteristic of the upper branch of a current-driven ionization wave.[12] The second, called magneto-deflagration, is a quasi-stationary mode that enables high exhaust velocities and, thus, I_{sp}. Magneto-deflagration is characterized by the lower branch of the wave. We review the theory and present an experimental characterization of these modes while the thruster is operating on the N_2 propellant. Finally, we show how propellant loading and flow collisionality can be used to enable reliable mode selection within the thruster.

II. DUAL MODE PLASMA THRUSTER

A. Facility description

The Stanford hydromagnetic thruster operates by ionizing and accelerating the propellant using an induced Lorentz force. The device, along with other pulsed Lorentz accelerators, is an extension of the original Marshall plasma gun.[14] Since their inception, Marshall guns have been used for applications ranging from simulated astrophysics,[15] plasma jet driven magneto-inertial fusion (PJMIF),[16] z-pinch schemes,[17] material ablation,[18] and even neutron production.[19] Despite studies in the 1960s on the potential use of these hydromagnetic plasma guns in space propulsion,[20] there has been little effort since the dawn of diverse electric propulsion demonstrations (1980s) to develop them as a source of thrust for space propulsion.

What makes hydromagnetic plasma guns unique among thrusters is that they are designed to operate with much higher voltages (~20 kV) and peak currents (~100 kA). These conditions can help overcome many of the operational problems that plague other electromagnetic thrusters such as the loss of flow stability and weak levels of plasma compression. For instance, higher operational voltage and currents have been shown to enable higher plume compression, acceleration, and even the ability to process and ionize complex molecular propellants.[15,21] The higher exhaust velocities, in particular, have even been shown to enable a prolonged operation in z-pinch schemes by stabilizing hydromagnetic instabilities through shear-flow effects.[17,21–23]

The hydromagnetic gun that we have studied is composed of three distinct systems that synergize to produce thrust: (1) an acceleration volume, (2) pulsed-power circuitry, and (3) a neutral gas injector. The acceleration volume of our device consists of a 26 cm long and 5 cm diameter coaxial segment with a 0.5 cm diameter copper cathode and rodded stainless-steel anodes.[15] Energy is supplied to the gun using a $56\,\mu F$ capacitor bank that can be charged up to 20 kV and supply peak currents of up to ~100 kA over $\sim 20\,\mu s$. This current flow induces magnetic field strengths of ~0.1–1 T within the coaxial segment that cause Lorentz forces to accelerate and compress the ionized propellant stream.

To initiate a discharge, neutral gas is injected into the accelerator using a fast rise-rate, variable mass-bit puff valve.[24] The thruster volume is maintained at rarefied conditions ($\sim 10^{-7}$ Torr) between discharge sequences by connecting it to a vacuum chamber that is equipped with a set of cryogenic pumps. The valve operates according to the principle of diamagnetic repulsion and allows the injection of ~10–100 mg of the propellant (e.g., N_2) over $\sim 300\,\mu s$. As the propellant reaches a critical breakdown density (i.e., the Paschen breakdown), it is rapidly ionized and accelerated out of the thruster.

B. Theory

The operation of plasma guns has uncovered the existence of two distinct flow patterns that depend on their initial gas loading (Fig. 1).[12,25] When the coaxial volume is pre-filled with gas, a thin current sheet is observed to convect along the electrodes in a process called a "snow plow." This process relies on the propagating conduction zone to collide with upstream mass until the local temperature and electrical conductivity have increased enough to form a shock front. This is the traditional operational mode that is observed in PPTs and allows highly localized current densities to form that "plow" propellant in a thin sheet. If, however, the thruster is initialized in rarified conditions, as is possible with the Stanford hydromagnetic thruster, a second mode of the operation can be observed where a collimated and quasi-steady jet forms.[21,26]

The properties of the operational modes can be derived by considering a magnetic extension to the Rankine–Hugoniot (RH) theory.[27] In this model, two distinct current-driven ionization waves are predicted if external electrical energy can be added to the flow. A theoretical depiction of the structure and properties of these waves is shown in Fig. 1. The magneto-detonation wave, or upper-branch solution, propagates along the length of the

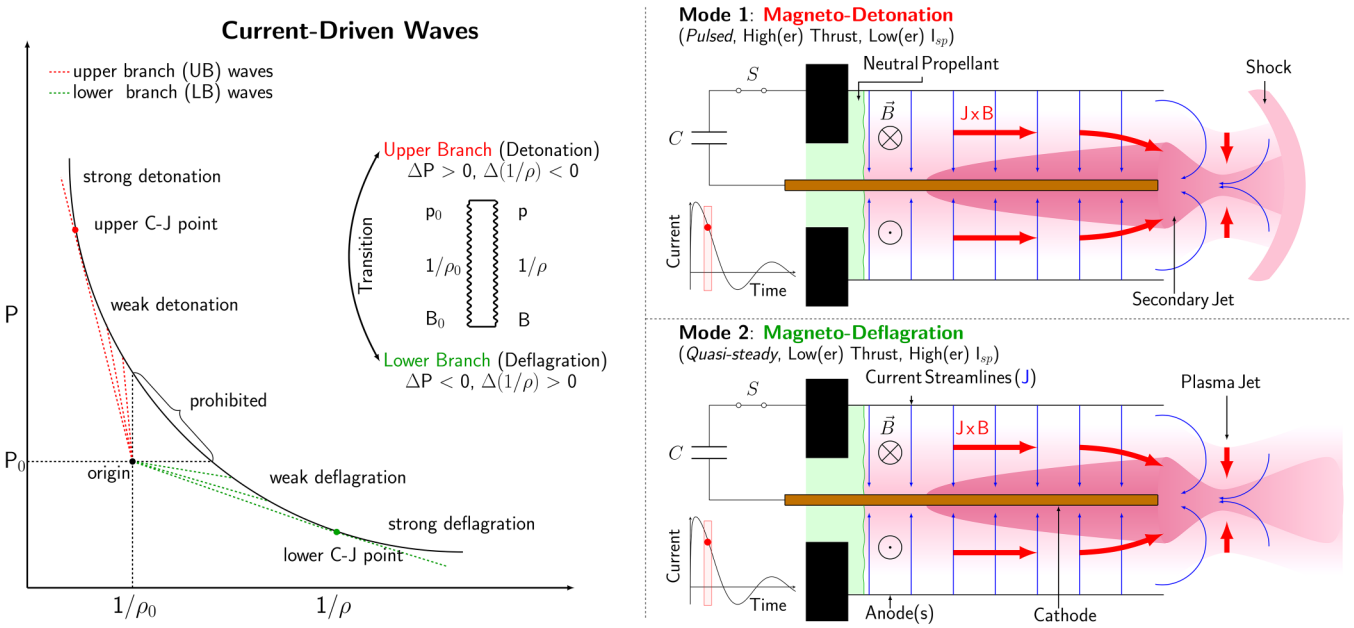

FIG. 1. Schematic depicting the operational modes of a hydromagnetic plasma thruster. The first mode, called a magneto-detonation wave, generates a transient shock that produces high(er) thrust and low(er) I_{sp}. The second mode, called a magneto-deflagration wave, generates a quasi-steady expansion wave that produces low(er) thrust and high(er) I_{sp}. The transition between these operational modes can be controlled by initializing the gasdynamic state of the thruster.

accelerator into the unprocessed gas while the magneto-deflagration wave, or lower-branch solution, is quasi-steady and propagates upstream toward the point where the propellant is fed in. The validity of the RH model has been investigated in separate studies by measuring the propagation and density characteristics of each wave and comparing that to theoretical predictions. The RH theory was found to agree to within 8% of measured propagation speeds and correctly predict that the deflagration mode is able to achieve higher exhaust velocities while the detonation mode is capable of processing larger instantaneous mass bits.[12]

Although effective at describing the existence of dual hydromagnetic modes, the RH theory does not capture the nuances of how they form. More importantly, simplified conservative jump relations offer little insight into how the distinct modes might smoothly transition into each other. This is an important consideration in the design of an agile propulsion system that may rely on exploiting the properties of these two modes. In Secs. III and IV, we present a combination of experiments and simulations to systematically explore the role that gasdynamics plays in selecting the operational mode of the thruster.

III. CHARACTERIZATION

A. Experimental

Mode selectivity in the thruster was studied by incorporating additional circuitry to precisely control the initial distribution of the propellant before a discharge starts. A combination of H_2 and N_2 gas was used to illustrate how fill rates of propellant influence the selectivity and transition between operational modes. The tunability of properties within each mode and the range of performance at low mass bits were not considered. Specifically, discharges were unable to be initiated at delay times lower than the characteristic filling time (i.e., $\sim 200\,\mu$s for N_2) of the thruster where self-breakdown can be supported.

A triggerable spark gap was employed to isolate the charged capacitor bank from the thruster until a high voltage trigger pulse was supplied to it. An illustration depicting the timing diagram used to initialize a discharge is shown in Fig. 2(a). The neutral gas distribution was adjusted within the acceleration volume by changing the time delay between the start of the propellant flow and the discharge (referred to as the gas injection delay or the gas filling time). This delay can cause a smooth transition from a deflagration wave to a detonation wave, the latter of which is illustrated in Fig. 2(b).

The structural evolution of the plasma flow is shown in Figs. 2(c)–2(h) for H_2 gas filling times of 0 and 250 μs, respectively, with a charging energy of 1.4 kJ. The propellant was puffed into the accelerator with a plenum pressure of 45 psi. Each image is presented in false color and was acquired using an Imacon Ultra8 ICCD camera with a 20 ns exposure time. The discharge times, t_D, of Figs. 2(c)–2(e) and 2(f)–2(h) were selected to be at the same points during the first half period of the current waveform, as shown in Fig. 2(a). With no imposed time delay, the operation recovers the behavior of the accelerator operating in puff mode where the electrodes are energized prior to gas being introduced into the thruster, and a deflagration mode is formed. When the H_2 gas is allowed to expand into the accelerator volume for 250 μs, the

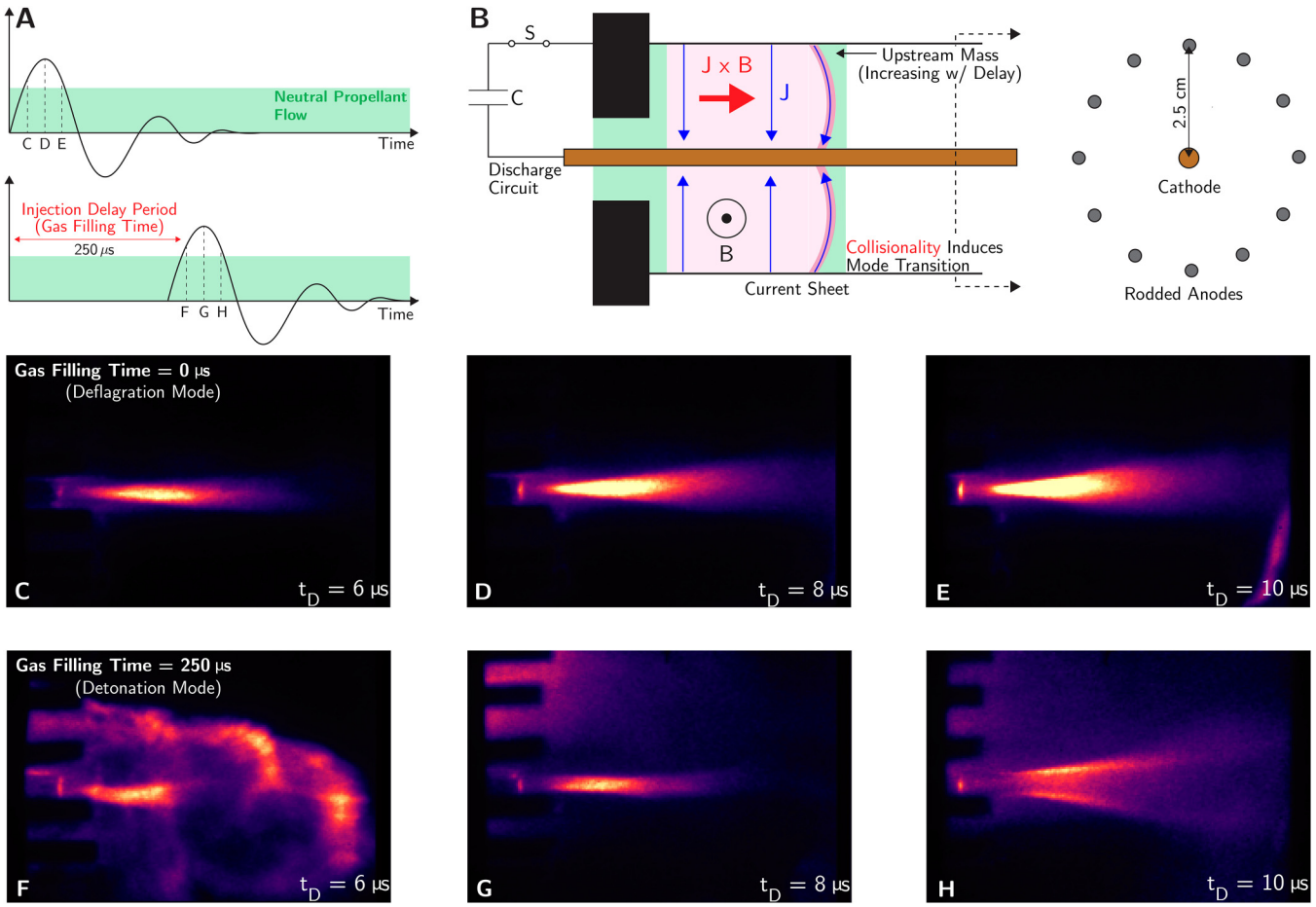

FIG. 2. The operational characteristics of the thruster can be changed by varying the distribution of the propellant within the acceleration volume. By increasing the delay between gas injection (H_2) and discharge initiation (a), the thruster can smoothly transition (b) from a deflagration wave (c)–(e) to a detonation wave (f)–(h). Eventually, increasing the upstream mass will induce a collisional shock as the ionization wave propagates through the propellant stream.

structure of the flow changes. For H_2, this time scale is sufficiently long to change the initial 10^{-7} Torr vacuum upstream condition throughout the 23 cm long electrode volume. The structure of the propagating front in Fig. 2(f) resembles that of a current sheet. The sensitivity of the ICCD also resolves an expansion wave immediately following the thin shock front. This observation is consistent with the Zeldovich model of a detonation wave as having a thin shock followed by a reaction zone and a trailing expansion wave.[28] Interestingly, as this detonation wave clears out of the channel, a second deflagration occurs during the second swing of the voltage ringdown [Figs. 2(g) and 2(h)].

1. Stagnation energy

The directed energy content of the plasma plume is one important metric that can lend insight into the operational transition and thrust capacity of the device. Detailed magnetohydrodynamic simulations of the thruster have shown that the kinetic energy contribution $(1/2\rho V^2)$ to the directed energy of a plume $(\Gamma_\epsilon = \left[\frac{5}{2}p + \frac{1}{2}\rho V^2\right]V)$ can be >5 times larger than the thermal contribution.[18,25] To assess this energy, a tungsten target was placed 4 cm downstream of the accelerator. The target was 2 cm in diameter, 0.5 cm thick, and mated to a thermally insulating base to center it in the vacuum tube. A 0.5 mm diameter fast type K thermocouple was attached to the backside of the target and connected to an alloy matched vacuum feedthrough to measure the bulk temperature rise, as illustrated in Fig. 3(a).

The stagnation energy measurements as a function of gas filling time is shown in Fig. 3(b). The thruster was charged to 1.4 kJ for each shot and the current and voltage traces remained unchanged with increasing injection delay. The energy transfer was calculated by taking the peak temperature rise experienced by the target of known mass, $E = mc_p\Delta T$. Separate trials were conducted for both H_2 and N_2 gas with injection delays of up to 800 μs with an interval of 50 μs.

The first set of data points, shown as occurring at negative gas filling times (or injection delays) in Fig. 3, corresponds to conditions

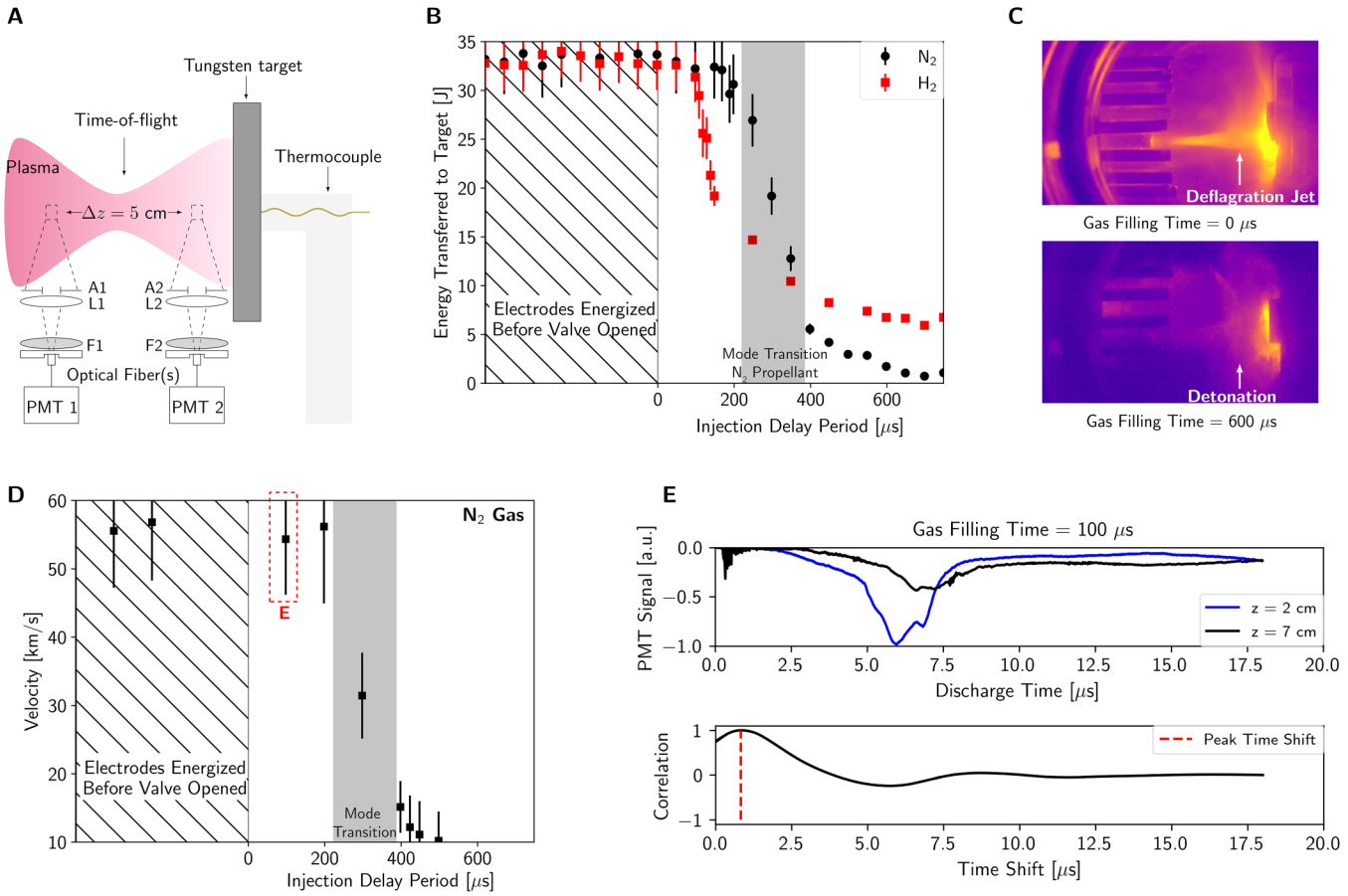

FIG. 3. (a) Experimental setup used to measure the stagnation energy and exhaust velocity of the plasma plume. (b) and (c) The energy transfer during stagnation smoothly decays with increasing injection delay. (d) and (e) Time-of-flight exhaust velocity measurements of the plasma plume. Gas filling times below the characteristic filling time (~200 μs for N_2) create a discharge when enough propellant enters the thruster to support self-breakdown.

where the electrodes were energized before gas was injected. After the gas is injected, it takes a characteristic filling time to reach a critical density in the thruster that supports self-breakdown. Gas filling times lower than the characteristic filling time also resulted in conditions where the electrodes are energized before the gas was injected. With increasing injection delay beyond that, a noticeable reduction in the directed energy content of the flow was recorded. The rate of the energy decay was found to also depend on the type of the propellant used. H_2 was observed to begin decaying sooner and with a larger characteristic slope than N_2. This suggests that gasdynamic expansion of the propellant plays a prominent role in determining the mode of the thruster. Evidence of a mode transition was also found by taking ICCD images at two extremes of gas filling time (0 and 600 μs), as shown in Fig. 3(c).

2. Exhaust velocity

Time-of-flight measurements were performed to quantify the effect of propellant loading on the acceleration efficiency of the thruster. Measurements with N_2 as a propellant were made to simulate conditions of interest for air-breathing applications. Two Hammatsu 1P28 photomultiplier tubes (PMTs) were placed 3 cm downstream of the electrodes and 5 cm apart to the visualize the propagation of the plume [Fig. 3(a)]. Each PMT was configured to feature a gain of 10^6, a rise time of ~30 ns, and a circular aperture of ~1 mm to limit spatial smearing. The acquired PMT traces for a gas filling time of 100 μs and a charging energy of 1.4 kJ are shown in Fig. 3(e). From these results, a cross-correlation function was employed to quantify the time delay between detector signals and remove any systematic bias in interpretation [Fig. 3(e)]. The measured time delay, Δt, was used to calculate the plume velocity knowing the spacing between detectors, $V = 5\,\text{cm}/\Delta t$.

The plasma flow velocity as a function of injection delay is shown in Fig. 3(d). As with the temperature rise measurements, the thruster's exhaust velocity was found to decrease with a similar slope. With a vacuum initial condition, the velocity was found to be approximately 55 km/s (I_{sp} ~ 5500 s). As gas expanded into the accelerator volume, that reduced to 11 km/s (I_{sp} ~ 1100 s). Thus,

the change in flow structure and localization is also accompanied by a reduction in the acceleration efficiency. These measurements indicate that propellant injection delay offers a controllable way to smoothly transition from processing larger mass bits (generating more thrust) to more efficiently using the propellant (generating more I_{sp}). The velocity measurement, while subject to uncertainties in relating propagating fronts of broadband emission to the bulk plasma velocity, is in general agreement with previous measurements made on the thruster based on immersed Mach probes,[12] as well as schlieren videography.[22]

B. Monte Carlo simulation

A direct simulation Monte Carlo (DSMC) technique was used to explore how gas filling time (injection delay) influences the distribution of the propellant within the thruster, and, for purposes of estimating performance, the amount of the propellant mass that is processed by the discharge (i.e., the mass bit), with varying gas filling time. DSMC codes are popular methods for simulating rarefied flows and have been described in detail elsewhere.[29,30] In the system presented here, N_2 was simulated in a 2D space within an axisymmetric region modeled after the coaxial thruster. Rotational and vibrational degrees of freedom of the gas were ignored. Gas-surface interactions and reflections off of the thruster walls were computed using the Maxwell model with an accommodation coefficient of 0.7. This value was selected based on experimental measurements.[31] The gas-puff valve was treated as a source reservoir of particles maintained at constant pressure and connected to the nozzle entrance. At each time step, a set of particles was initialized within the reservoir volume, with positions and velocities corresponding to a uniform Maxwellian distribution at a pressure of 45 psi and temperature of 293 K.

To capture the collisional dynamics of gases in DSMC methods, the time step and cell size must be chosen to resolve the minimum collision frequency and collisional mean free path. These requirements become prohibitive in this case as the neutral gas expands from a valve pressure of 45 psi to vacuum ($\sim 10^{-7}$ Torr) conditions. To overcome this, free molecular flow was assumed everywhere, and particles were only allowed to interact with boundary surfaces. For a diatomic molecule like N_2, the particle flux in the hydrodynamic regime (with collisions) is larger than that of the free molecular regime by a factor of 1.414.[32] We therefore expect our DSMC results to underpredict the mass flux into the gun by a similar amount. A complete overview of the numerical procedure and description of the assumptions is provided in Ref. 31.

Results of the neutral gas simulations at select times during the gas expansion process are shown in Fig. 4. The simulation region is initiated to be in high vacuum. At t = 0, the valve is opened, and particles begin to enter the domain through the nozzle. The valve remains open for 300 μs to be consistent with prior experimental characterizations of the puff valve. At each time step, the neutral gas distribution within the gun volume was integrated and recorded to capture its behavior as a function of gas filling time. Finally, the integrated mass upstream of the ionization plane is plotted against experimental results of velocity in Fig. 4(a). Here, the ionization plane was assumed to be the first axial point within the acceleration volume where the gas is simultaneously exposed to both electrodes with a pressure that can support breakdown.

The gasdynamic simulations show agreement between the time scales over which gaseous expansion impacts thruster performance (Fig. 3) and the slope by which those changes occur. Not only that, they also offer insight into how the operational mode of the thruster can be selected. For instance, a steady magneto-deflagration requires a smooth expansion process to transition from a region of higher pressure and density to a lower one. This means that the flow must remain weakly collisional as it accelerates out of the thruster. To predict the transition between these regimes, we assume a propagating current sheet (reaction zone) convects downstream with velocity V. Flow transition occurs when this current sheet narrows to form a collisional shock. We describe this

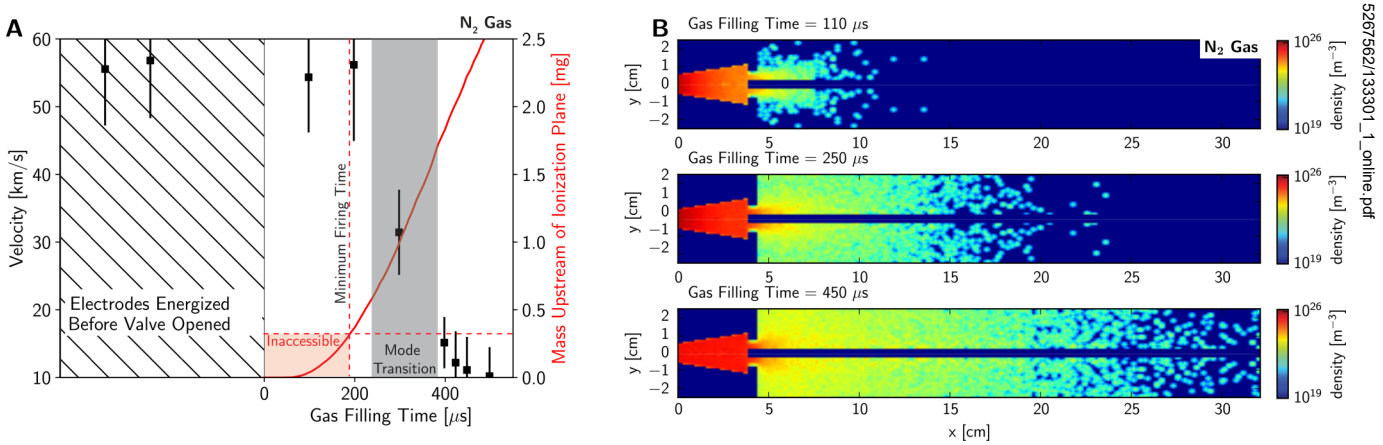

FIG. 4. (a) Comparison of the measured exhaust velocity and (b) simulated the N_2 propellant distribution in the thruster as a function of the delay between gas injection and the beginning of a discharge. An increasing gas filling time (injection delay) results in a more collisional upstream condition for the ionization wave to propagate into. Gas filling times below $\sim$200 μs are not accessible as there is an insufficient propellant in the thruster to support self-breakdown.

process by assuming upstream neutrals that enter the reaction zone are immediately ionized. These streaming ions, with initial speed $V_r = V$ relative to the current sheet, will then experience a relaxation process proportional to the ion-ion collision frequency, ν_{ii},

$$\frac{dV_r}{dt} = -\nu_{ii} V_r, \tag{1}$$

after which they will be stationary with respect to the current sheet. The characteristic relaxation time and distance of this process are $\tau_s = 1/\nu_{ii}$ and $\lambda_s = V\tau_s$, respectively.

When there is no injection delay, the upstream condition is constrained to be 10^{-6}–10^{-7} Torr by cryopumps ($n_n \sim 10^{16}$ m^{-3}). In these conditions, there is no way for the current sheet to further narrow (through an increasing entrained ion density, higher conductivity, higher ion temperature, and thus a higher ion-ion collision frequency) as it propagates into vacuum. Increasing gas filling time, however, fuels the narrowing of the current sheet and enables the transition to the detonation regime. For instance, assuming an average convective velocity of $V \sim 10$ km/s and $T \sim 10$ eV, the relaxation length exceeds 1 cm at $n_p \sim 10^{20}$ m^{-3}.[33,34] In this way, the neutral gas simulations start predicting collisionally induced mode transitions become possible with as little as ∼250 μs of injection delay while operating with the N_2 propellant. Any further delays past that will impact the strength of the detonation wave.[12]

IV. THRUSTER PERFORMANCE

The characterization results can be combined to estimate the performance metrics of each operating mode and the tunability range between them. The depth of the tunability range can be optimized by considering the propellant flow control options that are available in PPT architectures. For instance, as shown in Fig. 5, the maximum rate of the propellant flow, discharge (pulse) rate, gas filling time, and gas valve opening frequency can all be independently changed on demand. These changes can enable mode transitions to occur that feature distinct time scales, properties, and performance. For instance, the DSMC results for a single injection, Fig. 4, show that the accelerated mass bit can be tuned depending on the time that the propellant is allowed to expand into the acceleration volume. This introduces a trade-off between I_{sp} and thrust that can be adjusted between discharge pulses of the thruster. After a gas filling time of ∼210 μs, the available mass bit of N_2 (that can be processed) is ∼0.4 mg while the exhaust velocity is at its highest, ∼55 km/s. After a gas filling time of ∼450 μs however, the exhaust velocity drops to ∼11 km/s while the available mass bit increases to >2 mg. We quantify the effect of gasdynamic tunability and dual mode operation on thruster performance with fixed input power and propellant mass flow rates. In this case, mode transitions can occur in the thruster by allowing more propellant to fill the acceleration volume (e.g., higher gas filling time).

A. Preliminary performance tunability—Fixed input power and mass flow rate

To characterize potential performance, we assume that the hydromagnetic thruster operates in a burst mode with an average input power of 1.4 kW. Each thrust event (referred to as a pulse) follows from the characterization results presented in Figs. 2–4, namely, each consumes 1.4 kJ of energy and lasts ∼20 μs. The propellant is introduced using the same gas puff valve (and mass flow rate) over 1 ms with enough propellant to fuel consecutive pulse events (referred to as a burst). These pulses are then uniformly distributed across the gas-puff opening (ranging between 2 and 5 events depending on the gas filling time) to utilize the propellant. The instantaneous mass bit available for each pulse is assumed to follow from the DSMC characterization of single pulses in Fig. 4 and is a function of the gas filling time in the accelerator. Uncertainties in the simulated gas distribution will linearly increase the uncertainty in the preliminary thruster performance metrics (e.g., thrust and propulsive efficiency).

In extrapolating from single pulses to burst operation, the performance of each pulse is assumed identical. From this, the average thrust (F_T) can be calculated by

$$F_T = (\Delta m) V N_p f_{\text{valve}} \eta_m, \tag{2}$$

where Δm is the instantaneous mass bit for a single pulse, V is the measured exhaust velocity of the plume, N_p is the number of pulses per valve opening, and f_{valve} is the opening frequency of the

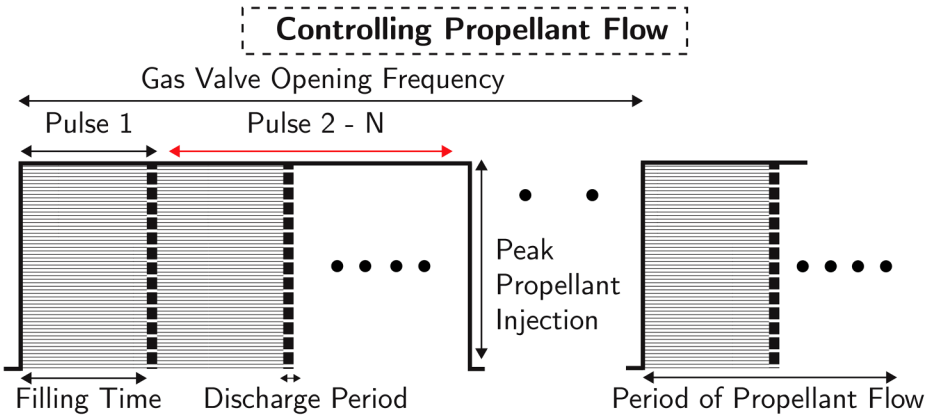

FIG. 5. Schematic illustrating the dynamics of propellant injection (period of propellant flow) and discharge initiation (filling time + discharge period) in a dual mode hydromagnetic thruster. Gasdynamic control could involve independently changing the peak rate of the propellant flow, gas filling time, discharge (pulse) duration, number of pulses/valve opening, and valve opening frequency. Together, these properties could rapidly transition the operational mode of a thruster and change its performance.

gas puff valve. All these parameters are functions of the gas filling time and are inferred from the time-of-flight experiments and the DSMC simulations. The remaining parameter, η_m, is a measure of the mass utilization of the propellant stream. It quantifies the fraction of the available propellant mass that is moving at the measured exhaust velocity.

The variation of mass utilization with an increasing gas fill time is estimated using a combination of the velocity and stagnation energy measurements in Fig. 3 and the mass bit calculations in Fig. 4. We estimate the variation in η_M by comparing the kinetic energy of the plume ($1/2\ \Delta m\, V^2$) to the measured stagnation energy (i.e., ~33 J for the N_2 propellant with a gas filling time of ~210 μs). This yields a lower limit to the thruster mass utilization ranging from ~4.3% with gas filling times of ~210 μs to ~3% after 450 μs. It is important to note that flow dissipation effects, boundary layer effects, and the finite size of the stagnating body (2 cm) mean that all of the energy in the plume cannot be captured. We estimate these effects using numerical simulations to predict an upper bound on mass utilization in the thruster in Fig. 6.[18]

The performance of a hydromagnetic thruster operating on the N_2 propellant with a fixed valve opening period of 1 ms and a fixed input power is shown in Fig. 6. The gas-puff valve opening frequency (f_{valve}) is calculated to constrain the average input power of the thruster to be 1.4 kW while the number of pulses (N_p) is calculated based on the gas filling time required for each discharge. From Fig. 6, the average thrust and propulsive efficiency P_t/P_{in} (where $P_t = .5\Delta\, mV^2 f_{valve} N_p \eta_m$) are all tunable between two distinct modes. The first mode, which occurs at low gas filling times ($< \sim 220\,\mu$s), is a deflagration that offers high exhaust velocities (~55 km/s) and propulsion efficiency. The second mode, a detonation, can be generated by simply allowing the gas to expand into the accelerator longer (or by injecting more propellant) and offers high levels of average thrust.

The performance characterization in Fig. 6 indicates a tunability range of up to ~22% of the average thrust (at a constant operational power and mass flow rate) due to changes in the propellant filling time. The maximum achievable efficiency using the energy stagnation measurements to estimate η_m is ~15%. Although this is a reasonable limit of propulsive efficiency, we note the Stanford

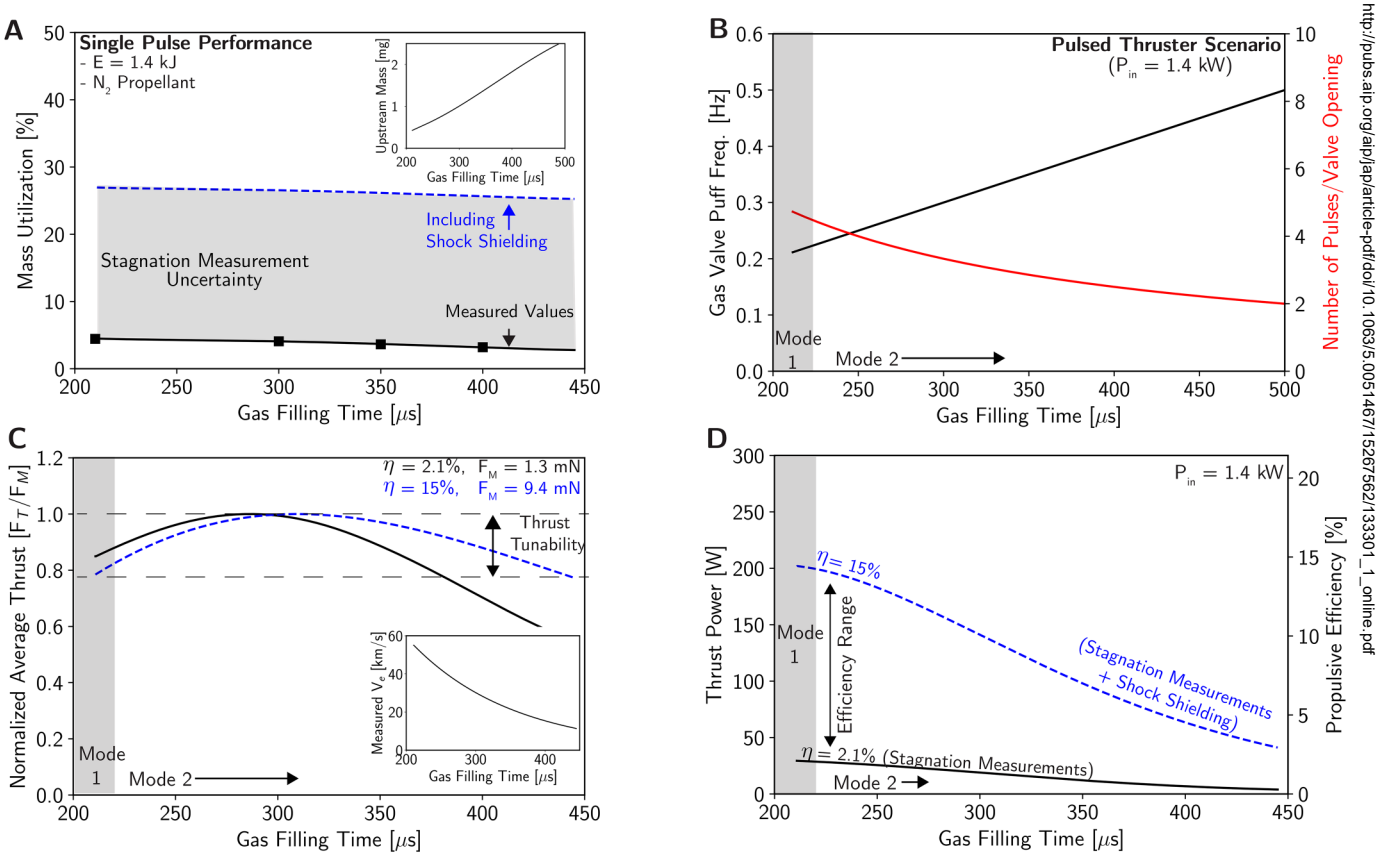

FIG. 6. Potential operational characteristics of a multi-mode thruster with an average input power of 1.4 kW, (a) mass utilization, (b) gas-puff valve dynamics, (c) thrust, and (d) efficiency. Each N_2 gas puff is assumed to remain open for ~1 ms and supply enough propellant for N_p uniformly distributed discharge events (pulses). The results assume the measured velocities and processed mass remain constant between discharge events (Fig. 4). The amplitude of the thrust tuning range depends on the properties of the gasdynamic injection (e.g., amplitude, rate, filling time, etc.) and can be optimized depending on the application.

geometry and operational characteristics have not been optimized. It is noteworthy that despite the lower limits based on our measured stagnation energy experiments, versions of these plasma sources operating in deflagration conditions (i.e., mode 1) at high pulse energies (30 kJ),[35] seem to have exhibited propulsive efficiencies above 50% (measured using a fish-trap pendulum thrust stand).

B. Limitations

Considerable work still needs to be done to understand the performance characteristics (i.e., thrust vs specific impulse) of operational modes in thrusters of different size, energy, propellant type, and discharge time scale. For example, projections described in Fig. 6 are limited by the accuracy of mass utilization within the thruster. Accurately identifying how much propellant is left inside the acceleration channel and how much propellant convects at lower velocities still requires considerable research in PPTs. In addition, quantifying the variation in performance across many shots is also important to establish the scalability of the dual mode operation. Even with these uncertainties, Fig. 6 offers bounded estimates of thruster performance and gives insight into how a dual mode operation can be achieved in future thrust technologies. The claim of thrust tunability is supported by previous experimental characterizations of PPTs that showed anomalous increases in thrust are possible with an increasing mass bit.[13]

This study focuses on exploring performance tunability in conditions where Rankine–Hugoniot mode transitions occur. There is, however, a considerable range of conditions (i.e., mass bits) within each mode that have not been considered in this work. Specifically, due to limitations caused by self-breakdown, mass bits lower than ∼0.1 mg (Fig. 6) were not possible to characterize experimentally. Previous studies of lower pulse energy PPTs (with the same specific enthalpy) showed that decreasing mass bits resulted in increasing exhaust velocities and lower levels of average thrust.[13] These conditions are representative of the deflagration mode described in this paper and offer a parameter space where higher impulse bit and thrust tunability might be possible.

V. CONCLUSION

This paper describes a novel hydromagnetic thruster that can operate in two distinct modes. These modes have performance characteristics that can enable the thruster to rapidly transition from optimizing thrust generation to propellant utilization. A theory is presented to describe the structure and evolution of each mode along with motivating the exploration of gasdynamics as a controllable means to enable reconfigurability in thrusters. A combination of rarefied simulations, experiments, and collisionality estimates supports this theory and establishes baseline performance metrics for a hydromagnetic thruster and a parameter space over which mode transitions can be expected to occur.

The characterization of a preliminary thruster is given to illustrate how gasdynamic control can be used and optimized for EP technology. These measurements are not intended to communicate propulsive or tunability properties of an optimized design. Instead, we hope to motivate research efforts to identify and refine the performance metrics, tunability range, and applicability of the dual mode operation in new and existing propulsion technologies. There remain considerable scientific and engineering challenges that must be solved before dual mode control can be implemented in EP technology on a commercial scale. For example, separate studies focusing on the effect of discharge energy, geometry, voltage, and propellant composition on the performance of each mode still need to be performed. Direct measurements of thrust will also reduce uncertainties in estimating mass utilization and improve understanding of performance tunability, such as the trade-off between thrust and I_{sp}. Finally, testing the dual mode operation in representative air-breathing environments where harvested propellant feeds can be leveraged still needs to be demonstrated.

AUTHORS' CONTRIBUTIONS

M.A.C. and T.C.U. conceived the idea of a dual mode thruster. T.C.U. and W.M.R. performed the experiments. T.C.U. analyzed the experimental results. W.M.R. performed the gasdynamic simulations. T.C.U. and M.A.C. wrote the manuscript. W.M.R. described the gasdynamic results.

ACKNOWLEDGMENTS

This research is supported by the U.S. Air Force Office of Scientific Research, with Dr. Mitat Birkan as Program Manager. The authors wish to acknowledge Hadland Imaging for generously providing an Imacon ICCD camera to visualize the dynamics of the coaxial plasma flow.

DATA AVAILABILITY

The data that support the findings of this study are available from the corresponding author upon reasonable request.

REFERENCES

[1]M. Peukert and B. Wollenhaupt, in *EPIC Workshop, Brussels* (European Space Agency, 2014).
[2]S. Mazouffre, Plasma Sources Sci. Technol. **25**, 033002 (2016).
[3]J. S. Snyder and R. R. Hofer, "Throttled performance of the SPT-140 hall thruster," AIAA Paper No. 2014-3816, 2014.
[4]G. Cifali, T. Misuri, P. Rossetti, M. Andrenucci, D. Valentian, and D. Feili, "Preliminary characterization test of HET and RIT with nitrogen and oxygen," AIAA Paper No. 2011-6073, 2011.
[5]A. Gurciullo, A. L. Fabris, and M. A. Cappelli, J. Phys. D: Appl. Phys. **52**, 464003 (2019).
[6]P. Dietz, W. Gärtner, Q. Koch, P. E. Köhler, Y. Teng, P. R. Schreiner, K. Holste, and P. J. Klar, Plasma Sources Sci. Technol. **28**, 084001 (2019).
[7]F. Romano, B. Massuti-Ballester, T. Binder, G. Herdrich, S. Fasoulas, and T. Schönherr, Acta Astronaut. **147**, 114 (2018).
[8]F. Romano, Y.-A. Chan, G. Herdrich, C. Traub, S. Fasoulas, P. Roberts, K. Smith, S. Edmondson, S. Haigh N. Crisp *et al.*, Acta Astronaut. **176**, 476 (2020).
[9]J. Ziemer and R. Petr, "Performance of gas-fed pulsed plasma thrusters using water vapor propellant," AIAA Paper No. 2002-4273, 2002.
[10]A. Larson, T. Gooding, B. Hayworth, and D. Ashby, AIAA J. **3**, 977 (1965).
[11]J. Mather, Phys. Fluids **7**, S28 (1964).
[12]K. T. Loebner, T. C. Underwood, and M. A. Cappelli, Phys. Rev. Lett. **115**, 175001 (2015).
[13]J. K. Ziemer, "Performance scaling of gas-fed pulsed plasma thrusters," Ph.D. thesis (Princeton University, 2000).

[14]J. Marshall, Phys. Fluids **3**, 134 (1960).
[15]T. C. Underwood, K. T. Loebner, and M. A. Cappelli, High Energy Density Phys. **23**, 73 (2017).
[16]Y. F. Thio, S. C. Hsu, F. D. Witherspoon, E. Cruz, A. Case, S. Langendorf, K. Yates, J. Dunn, J. Cassibry, R. Samulyak *et al.*, Fusion Sci. Technol. **75**, 581 (2019).
[17]U. Shumlak, R. Golingo, B. Nelson, and D. Den Hartog, Phys. Rev. Lett. **87**, 205005 (2001).
[18]T. C. Underwood, V. Subramaniam, W. M. Riedel, L. L. Raja, and M. A. Cappelli, Fusion Eng. Des. **144**, 97 (2019).
[19]Y. Zhang, U. Shumlak, B. Nelson, R. Golingo, T. Weber, A. Stepanov, E. Claveau, E. Forbes, Z. Draper, J. Mitrani *et al.*, Phys. Rev. Lett. **122**, 135001 (2019).
[20]J. K. Ziemer, *Electric Propulsion and Plasma Dynamics Lab Report* (Princeton University, 2000).
[21]T. C. Underwood, K. T. Loebner, V. A. Miller, and M. A. Cappelli, Sci. Rep. **9**, 1 (2019).
[22]T. C. Underwood, K. T. Loebner, V. A. Miller, and M. A. Cappelli, Exp. Fluids **61**, 162 (2020).
[23]U. Shumlak, B. Nelson, E. Claveau, E. Forbes, R. Golingo, M. Hughes, R. Oberto, M. Ross, and T. Weber, Phys. Plasmas **24**, 055702 (2017).
[24]K. T. Loebner, T. C. Underwood, and M. A. Cappelli, Rev. Sci. Instrum. **86**, 063503 (2015).
[25]V. Subramaniam, T. C. Underwood, L. L. Raja, and M. A. Cappelli, Plasma Sources Sci. Technol. **27**, 025016 (2018).
[26]K. T. Loebner, B. C. Wang, F. R. Poehlmann, Y. Watanabe, and M. A. Cappelli, IEEE Trans. Plasma Sci. **42**, 2500 (2014).
[27]D. Y. Cheng, Nucl. Fusion **10**, 305 (1970).
[28]J. von Neumann John, A. H. Taub, "Theory of detonation waves. Progress Report to the National Defense Research Committee Div. B, OSRD-549, (April 1, 1942. PB 31090)." John von Neumann: Collected Works 1957 (1903).
[29]I. D. Boyd and T. E. Schwartzentruber, *Nonequilibrium Gas Dynamics and Molecular Simulation* (Cambridge University Press, 2017), Vol. 42.
[30]F. J. Alexander and A. L. Garcia, Comput. Phys. **11**, 588 (1997).
[31]A. Eggleton and F. Tompkins, Trans. Faraday Soc. **48**, 738 (1952).
[32]H. W. Liepmann, J. Fluid Mech. **10**, 65–79 (1961).
[33]E. C. Merritt, A. L. Moser, S. C. Hsu, C. S. Adams, J. P. Dunn, A. Miguel Holgado, and M. A. Gilmore, Phys. Plasmas **21**, 055703 (2014).
[34]T. C. Underwood, *Hydromagnetic Stability and Collisional Properties of Current-Driven Plasma Jets* (Stanford University, 2019).
[35]D. Y. Cheng, AIAA J. **9**, 1681 (1971).